

Framework for Low-Temperature Cracking Analysis of Asphalt Mixtures Using a Viscoelastic Continuum Damage Model

Marcelo S. Medeiros Jr., Ph.D.¹; Jo Sias Daniel, Ph.D., P.E., M.ASCE²; and Ghassan R. Chehab, Ph.D.³

Abstract: Thermal cracking performance assessment of flexible pavements is paramount to improve the quality of the roads in cold-climate regions. In this paper, a reduced testing framework for analysis of hot-mix asphalt (HMA) concrete is proposed to replace the indirect tensile (IDT) creep compliance and strength testing by dynamic modulus and fatigue tests performed on an asphalt mixture performance tester (AMPT) device. The theoretical aspects of the methodology are shown as well as its validation with laboratory results. Mixtures containing various percentages of reclaimed material (RAP) were investigated to assess the adequacy of the proposed method to this type of material. Results showed that the proposed framework can be successfully used to predict the low-temperature creep compliance and IDT strength, which are the two key elements in thermal cracking performance analysis of flexible pavements. DOI: 10.1061/(ASCE)MT.1943-5533.0001215. © 2014 American Society of Civil Engineers.

Introduction

In regions where significant thermal cycling occurs, the strong incidence of low-temperature cracking is a major source of premature deterioration of flexible pavements and asphalt overlays. The mechanical and environmental loadings impose mainly longitudinal strains along the pavement due to its natural tendency to contract at lower temperatures. However, the movement is prevented by friction with the underlying layers, causing the stresses to build up. During unfavorable environmental and traffic conditions, the forces acting on the surface layer overcome the tensile strength of the material, leading to the occurrence of top-down cracks (Haas et al. 1987). As the cracks evolve throughout the cold season, the water starts to infiltrate, thereby weakening the supporting layers of the pavement structure. Many studies have been conducted to better understand the key mechanisms behind this distress mode. Moreover, recent advances in fracture testing and modeling of hot-mix asphalt (HMA) materials (e.g., Wagoner et al. 2005; Kim et al. 2008; Underwood and Kim 2011) have addressed the problem using different approaches. The current Superpave specifications are based upon the linear viscoelastic analysis of both asphalt binders and mixtures. Despite not addressing some issues related to constitutive nonlinearities, this represents a major step forward towards the proper selection of materials in addition to a better assessment of the low-temperature performance of flexible pavements. Conversely, this approach imposed a higher level of sophistication on the material's testing protocol when compared to

previous pavement design guides. In most cases, the required tests are beyond the current technical capabilities of the practitioners. The objective of this paper is therefore two-fold. The first goal is to propose a reduced testing framework for the low-temperature viscoelastic material characterization, and the second is to use a continuum damage model that incorporates the nonlinear constitutive behavior of the HMA mixtures to propose a criterion that estimates the mixture's critical cracking temperature. Mixtures with varying percentages of reclaimed material (RAP) ranging from 0 to 40% were used in this study in order to verify the applicability of the proposed methodology to RAP mixtures.

MEPDG Thermal Cracking Analysis

The thermal-cracking prediction model (TCMODEL) used in the *Mechanistic-Empirical Pavement Design Guide* (MEPDG) was originally developed by Hiltunen and Roque (1994) and estimates the amount of thermal cracks (given as the total length of cracks per length of pavement) as a function of time. The model uses the material tensile strength as the threshold parameter for crack initiation and calculates the crack propagation using a linear-elastic fracture mechanics model based on a variation of the Paris law (Paris et al. 1961), adapted for a linear viscoelastic material. The inputs to the model are the creep compliance, tensile strength, coefficient of thermal contraction, pavement thickness, and pavement temperature along its depth. TCMODEL interprets the pavement as a layer of asphalt subjected to a tensile stress distribution with depth. It also assumes that the cracks are uniformly spaced; however, only one crack is modeled. A statistical transfer function is then used to predict the amount of thermal cracks in the field that are equal or greater than the thickness of the surface layer.

The TCMODEL uses the creep compliance, $D(t)$, as input for stress calculations at various depths into the pavement. This information is not used as is but converted to the relaxation modulus, $E(t)$, and then convolved with the thermal strain history by means of a convolution integral. The thermal cracks are considered to initiate when the tensile stresses exceed the tensile strength of the mixture. The temperature at which this failure happens is known as the critical cracking temperature. TCMODEL also uses the slope of the linear portion of the log compliance–log time master curve as one

¹Research Scientist IV, Louisiana Transportation Research Center, 4101 Gourrier Ave., Baton Rouge, LA 70808 (corresponding author). E-mail: marcelom@lsu.edu

²Associate Professor, Civil Engineering, Univ. of New Hampshire, Kingsbury Hall, Room W171 33, Academic Way, Durham, NH 03824. E-mail: jo.daniel@unh.edu

³Associate Professor, Civil Engineering, American Univ. of Beirut, Beirut, Lebanon. E-mail: gc06@aub.edu.lb

Note. This manuscript was submitted on March 14, 2014; approved on October 7, 2014; published online on December 16, 2014. Discussion period open until May 16, 2015; separate discussions must be submitted for individual papers. This paper is part of the *Journal of Materials in Civil Engineering*, © ASCE, ISSN 0899-1561/04014265(9)/\$25.00.

of the parameters in the assessment of the crack depth. A detailed description of the model's theoretical formulation can be found elsewhere (Hiltunen and Roque 1994).

The coefficient of thermal contraction is calculated based on the volumetric properties of the mixture as proposed by Jones et al. (1968) and the creep compliance and indirect tensile strength as per AASHTO T322-07 (AASHTO 2007). Creep tests are run in indirect tensile (IDT) mode at 0, -10, and -20°C, while the tensile strength test is performed at -10°C in IDT mode at a constant crosshead compression rate of 12.5 mm/min. The complete observance of this standard can only be achieved in a laboratory equipped with a controllable environmental chamber capable of reaching -20°C and a closed-loop servohydraulic testing machine. These requirements make the two tests impractical for most departments of transportation and contractors.

Interconversion between Linear Viscoelastic Properties

Interconversion of linear viscoelastic fundamental properties (also referred to as response functions) is achieved either analytically or numerically. Relationships between moduli and compliances are possible due to the fact that both are different ways to represent the material's time dependency. Furthermore, from a mathematical standpoint, linear viscoelastic properties are equivalent to one another for each mode of loading (such as uniaxial or shear) regardless of the excitation form (transient or steady state). The interconversion procedure starts with the curve fitting of the dynamic modulus, $|E^*(\omega)|$, to a sigmoidal function that allows for data extrapolation and smoothing.

The complex modulus now defined in the appropriate functional form is divided into its real and imaginary parts, usually called storage and loss functions, respectively. The storage modulus, E' , is then fitted to Eq. (1) using the multidata method (Cost and Becker 1970). This process was done over 19 decades of frequency in order to capture the entire viscoelastic response of the mixtures. The numerical method of interconversion devised by Park and Schapery (1999) was adopted in this work and is briefly explained as follows:

$$E' = |E^*| \cos(\varphi) = E_e + \sum_{i=1}^m \frac{\omega^2 \rho_i^2 E_i}{\omega^2 \rho_i^2 + 1} \quad (1)$$

where E_e = equilibrium modulus (MPa), E_i = relaxation strength (MPa), ρ_i = relaxation time (s), and ω = angular frequency (rad/s).

The set of constants comprised of E_e , E_i , and ρ_i (totalizing 39 constants) can be used to obtain the corresponding Prony coefficients for the creep compliance, $D(t)$, if a set of retardation times, τ_i , is assumed ($\tau_i = 2\rho_i$). This is done by simply solving the following linear system of equations represented using indicial notation. Note that in this work k and j ranged from 1 to 19

$$A_{kj} D_j = B_k \quad (2)$$

where

$$A_{kj} = E_e (1 - e^{-\frac{t_k}{\tau_j}}) + \sum_{i=1}^m \frac{\rho_i E_i}{\rho_i - \tau_j} (e^{-\frac{t_k}{\rho_i}} - e^{-\frac{t_k}{\tau_j}}) \quad (3)$$

and

$$B_k = \frac{1 - [E_e + \sum_{i=1}^m E_i e^{-t_k/\rho_i}]}{E_e + \sum_{i=1}^m E_i} \quad (4)$$

Based on this methodology, the uniaxial compressive complex modulus was converted to creep compliance, then compared to IDT

creep compliance measurements. This raises the question as to whether the two distinct modes of loading can interchangeably be used to substitute one another. As mentioned previously, no mathematical constraint exists that prevent the interconversion. Moreover, the work developed under phase III of the National Cooperative Highway Research Program (NCHRP) project 9-29 (Christensen and Bonaquist 2004) showed that IDT creep compliance tests yield results equivalent to those of creep compliance tests under uniaxial compressive stress. The coefficient of correlation (r^2) between the two was found to be 93%.

Viscoelastic Continuum Damage Model

Several constitutive models exist to describe the behavior of HMA, some of which are based on a micromechanical approach while others use the continuum damage theory. The model briefly described herein has been developed at North Carolina State University and consists of a simplified viscoelastic continuum damage model (Park et al. 1996; Daniel 2001; Chehab and Kim 2005; Underwood et al. 2009). It will be referred to as the VECD model from this point on.

The VECD model utilizes Schapery's nonlinear viscoelastic constitutive theory for materials with distributed growing damage (Schapery 1975; Park and Schapery 1997) and quantifies the damage magnitude by assessing the decrease in the effective stiffness observed as the variation on the slope of the instantaneous secant modulus. The damage is quantified by an internal state variable based on the work potential theory and accounts for microstructural changes within the material. The model utilizes the elastic viscoelastic correspondence principle to reduce the governing field and boundary equations of viscoelastic problems into a mathematical equivalent of those for elasticity problems.

The constitutive relationships are defined not in terms of actual strains but by pseudostrains, defined in Eq. (5)

$$\epsilon^R = \frac{1}{E_R} \int_0^t E(t-\tau) \frac{\partial \epsilon}{\partial \tau} d\tau \quad (5)$$

where ϵ^R = pseudostrains; ϵ = real strains, $E(t)$ = relaxation modulus; and E_R = reference modulus.

For transient temperature conditions, the variable time is replaced by the reduced time, $\xi(t)$, at each infinitesimal increment of temperature and is calculated using

$$\frac{d\xi(t)}{dt} = \frac{1}{a_T} \rightarrow \xi(t) = \int_0^t \frac{1}{a_T} dt \quad (6)$$

where the term a_T is the shift factor from the master curve construction. The shift factor is a material's fundamental property and can be mathematically represented in different forms. The VECD model is then represented by its three main components

$$W^R = W(\epsilon^R, S) \quad (7)$$

$$\sigma = \frac{\partial W^R}{\partial \epsilon} \quad (8)$$

$$-\frac{\partial W^R}{\partial S} = \frac{\partial W_s}{\partial S} \quad (9)$$

The state of stress in the material, σ , is given by an energy potential W^R , called the pseudostrain energy density function, which depends on a set of internal state variables S .

W_s accounts for the change in the irreversible energy (damage) due to changes in the material's microstructure (microcracking). Eq. (9) establishes the damage evolution rules, but cannot be

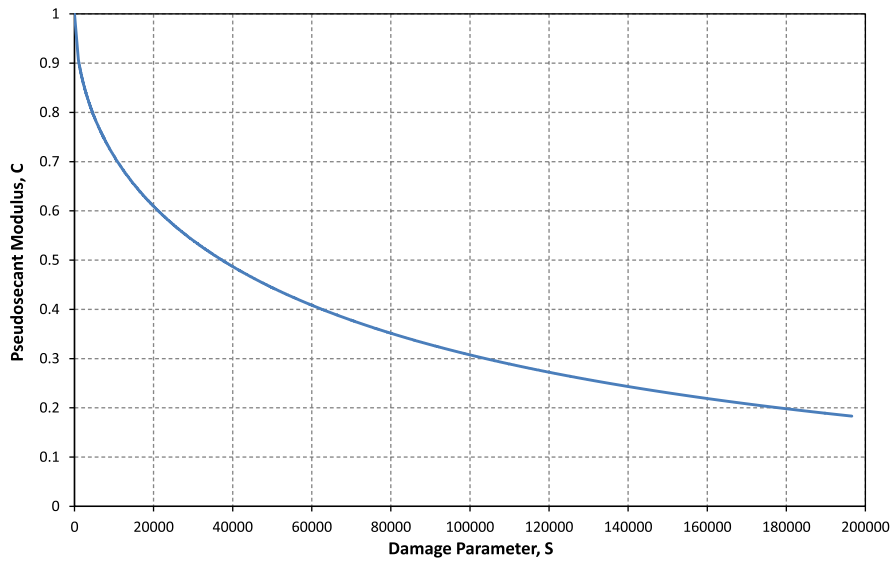


Fig. 1. Characteristic curve of NH PG 58 -28 20% RAP mixture

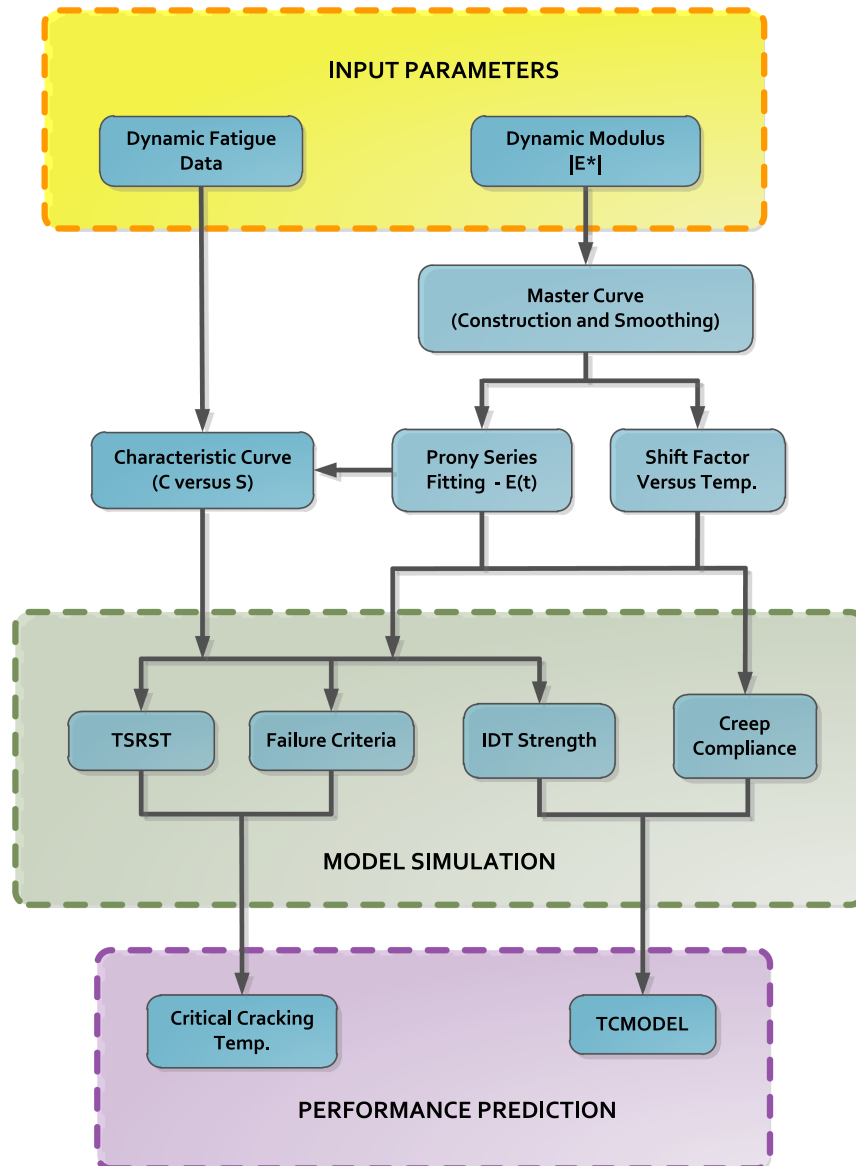


Fig. 2. Schematic diagram of the proposed methodology

$$W^R = \frac{1}{2} C(S) (\epsilon^R)^2 \quad (11)$$

directly used for viscoelastic media because the available force for growth of S and the corresponding resistance against its growth are both rate dependent for viscoelastic materials. A power law was then adopted to define the rate of damage evolution presented in Eq. (10), where the exponent α is obtained experimentally

$$\frac{dS}{dt} = \left(\frac{\partial W^R}{\partial S} \right)^\alpha \quad (10)$$

Schapery's correspondence principle guarantees that the stress can be defined in terms of a normalized pseudostrain modulus $C(S)$ that decreases as the damage evolves. The pseudostrain energy density function is defined as the area under the stress pseudostrain curve as given in Eq. (11)

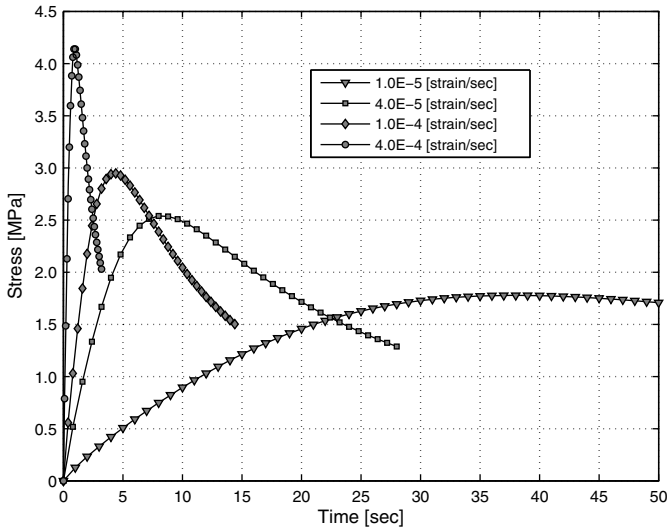


Fig. 3. Influence of different strain rates on the peak stress value

Table 1. Mixture Production Information

Production plant (PG grade)	NMAS (mm)	RAP content (%)	Total binder (%)	RAP binder (%)	VMA	VFA
NH (PG 64 -28)	12.5	0	5.7	0	17.5	64.3
		20	5.7	16.8	17.6	63.5
		30	5.7	25.2	17.3	64.8
		40	5.7	33.6	17.7	64.1
NY (PG 58 -28)	12.5	30	5.2	28.4	16.4	64.1
		40	5.2	37.7	16.8	62.5
NY (PG 64 -22)		0	5.2	0	16.4	64.1
		20	5.2	19.0	16.5	64.1
		30	5.2	28.4	17.1	62.9
		40	5.2	37.7	16.6	61.4
VT (PG 52 -34)	9.5	0	6.7	0	18.8	68.1
		20	6.8	16.00	18.3	70.2
		30	6.6	24.7	18.6	70.5
		40	6.6	32.6	19.1	70.1
VT (PG 64 -28)		0	6.5	0	19.1	67
		20	6.7	16.1	18.4	70.3
		30	6.6	24.5	18.4	69
		40	6.6	33.0	18.7	67.7

Note: NMAS = nominal maximum aggregate size; VFA = voids filled with asphalt; VMA = voids in mineral aggregate.

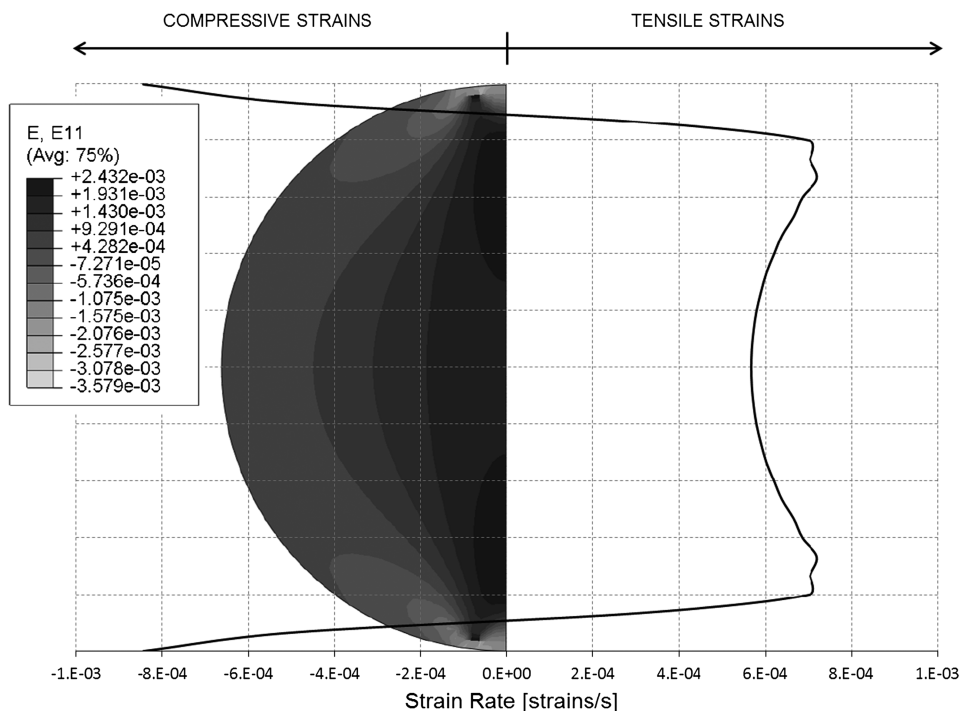


Fig. 4. Finite-element simulation of the IDT test

Table 2. Experimental Program

Test identification	Specifications	Temperature (°C)	Number of specimens
Dynamic modulus	AASHTO TP 79-12 (AASHTO 2012)	4, 20, 35	54
IDT creep	AASHTO T322-07 (AASHTO 2007)	0, -10, -20	54
IDT strength	AASHTO T322-07 (AASHTO 2007)	-10	54
Fatigue	Push-pull at 10 Hz	10	36
TSRST	AASHTO TP 10-93 (AASHTO 1993)	10/h	54

Table 3. Shift Factor Models

Model	Expression	Regression parameters
Polynomial	$\log_{10}(a_T) = A(\Delta T)^2 + B(\Delta T) + C$	$A, B,$ and C
WLF	$\log_{10}(a_T) = \frac{C_1(\Delta T)}{C_2 + (\Delta T)}$	C_1 and C_2
Exponential	$a_T = b e^{-\lambda(\Delta T)}$	b and λ

$$\sigma = \frac{\partial W^R}{\partial \epsilon} = C(S)\epsilon^R \quad (12)$$

The relationship between C and S is obtained experimentally and is shown in Fig. 1 for one of the mixtures evaluated in this work.

Proposed Methodology

Under the auspices of the NCHRP Project 9-29 (Christensen and Bonaquist 2004), the dynamic modulus, $|E^*|$, was chosen as the simple performance test for materials characterization and for flexible pavement structural design within the scope of the MEPDG. This effort set the basis for the design and construction of the asphalt mixture performance tester (AMPT). AMPT devices consist of relatively

small bottom-loading, servohydraulic devices equipped with a test chamber that serves as both the confining pressure cell and the automated environmental chamber (Bonaquist et al. 2003). The dynamic modulus test is performed in compressive uniaxial mode on nominal 100-mm-diameter, 150-mm-high cylindrical specimens cut and cored from gyratory compacted specimens. This system also allows for dynamic fatigue characterization (Kim et al. 2009) of the mixture, which can be used for nonlinear constitutive modeling.

The methodology proposed in this work consists of using the dynamic modulus and fatigue data from AMPT devices instead of the creep compliance and IDT strength employed in thermal crack performance evaluation. The VECD model presented earlier is used to estimate the critical cracking temperature of the mixture as well as the tensile strength using the AMPT dynamic modulus and fatigue data. Fig. 2 shows a schematic diagram of the proposed framework.

VECD Thermal Stress Calculation of the IDT Strength and Critical Temperature

Pseudostrains and stresses calculated using the VECD model were obtained using Eqs. (5) and (12), where the strain rates were selected according to the type of analysis. The input parameters were the $|E^*|$ from uniaxial compressive tests and tension-compression fatigue tests carried out on an AMPT device.

In Eq. (5), one can see that the relaxation modulus must be convolved (Kreyszig 2011) with the appropriate strain rate in order to calculate the pseudostrains; this process was accomplished numerically. Numerical computation of convolution integrals requires special attention regarding convergence, especially when recursive algorithms are employed. Several authors reported this problem and proposed different approaches to mitigate it (Taylor et al. 1970; Zocher et al. 1997; Mun 2006). This issue is greatly aggravated by the use of uneven time steps. That is the case when reduced times are used in lieu of actual time. Christensen (1982) presents an explicit numerical procedure to determine the solution of convolution integrals considering temperature variation. The method was reformulated to calculate pseudostrains using the following equations

Table 4. Summary of Errors from the Three Shift Factor Model Predictions

State (PG grade)	RAP content (%)	Polynomial		WLF		Exponential	
		Maximum error (%)	Minimum error (%)	Maximum error (%)	Minimum error (%)	Maximum error (%)	Minimum error (%)
NH (PG 64 -28)	0	N/A ^a	N/A ^a	N/A ^a	N/A ^a	N/A ^a	N/A ^a
	20	17.1	16.4	17.6	16.0	18.3	14.1
	30	3.9	2.8	4.3	3.3	4.9	0.4
	40	20.6	6.5	20.3	7.0	22.1	3.6
NY (PG 58 -28)	30	20.9	14.8	21.8	13.8	17.2	17.0
	40	4.2	1.2	4.6	0.8	3.0	1.3
NY (PG 64 -22)	0	11.6	8.5	11.1	9.0	13.4	5.4
	20	7.4	6.7	7.6	6.4	9.0	6.9
	30	0.5	0.2	1.2	0.6	4.0	1.9
	40	6.2	3.2	5.8	2.8	8.8	4.9
VT (PG 52 -34)	0	21.5	10.6	25.9	5.5	25.5	13.8
	20	25.3	13.0	29.7	7.8	17.8	17.8
	30	9.8	0.9	14.4	3.9	6.1	1.3
	40	10.3	7.7	19.2	16.8	1.3	0.7
VT (PG 64 -28)	0	31.8	18.5	32.6	17.6	28.4	20.9
	20	20.7	18.4	21.0	18.1	19.8	18.3
	30	N/A ^a	N/A ^a	N/A ^a	N/A ^a	N/A ^a	N/A ^a
	40	20.4	16.2	21.1	15.6	18.3	17.0

^aAssessment not available due to problems during creep testing.

$$\Delta t_q = t_q - t_{q-1}; \quad q = 1, \dots, p; \quad t_p = t; \quad t_0 = 0 \text{ (time interval discretization)}$$

$$\epsilon_R = \frac{1}{E_R} \left[E_e \epsilon(t) + \sum_{i=1}^{19} E_i F_p^{(i)} \right] \quad (13)$$

where

$$F_p^{(i)} = e^{(-\xi_p + \xi')/\rho_i} \left\{ F_{p-1}^{(i)} + [1 - e^{(-\xi_p + \xi_{p-1})/\rho_i}] \frac{\Delta \epsilon(t_p)}{\Delta t_p} (\rho_i/a_T) \right\}$$

After calculating the pseudostrains over the established time interval, the damage parameter was calculated using the recommendations found in Park et al. (1996) based on fatigue testing data

$$S = \left[\hat{S} \left(1 + \frac{1}{\alpha} \right) \right]^{1/1+\alpha^{-1}} \quad (14)$$

where \hat{S} is incrementally calculated using Eq. (10), assuming that before loading occurs S and C are 0 and 1, respectively. The time step i must be appropriately chosen such that no significant change in damage happens during the interval

$$\hat{S}_{i+1} = \hat{S}_i - 0.5(\Delta C)_i (\epsilon_R)^2 t^{1/\alpha} \quad (15)$$

IDT Strength

At low temperatures, the asphalt material has the tendency to fail in a brittle manner as opposed to the ductile behavior observed at intermediate and high temperatures. In IDT tests performed at temperatures below freezing, the tensile stress reaches its maximum value, then cracks initiate and abruptly propagate throughout the specimen, breaking it apart. This failure mechanism results in little or no residual strength after the peak (toughness). Therefore, in this study, the IDT tensile strength was considered as the peak value of the calculated stress curve [obtained from Eq. (12)]. Fig. 3 shows the output of the stress calculations at different strain rates.

A linear viscoelastic finite-element analysis of the IDT test using *ABAQUS version 6.11* was carried out to obtain the horizontal tensile strain rates. The actuator loading was simulated by a fixed displacement rate of the nodes corresponding to the area under the loading strip. A loading rate of 12.5 mm/min was used, following

Table 5. Creep Compliance Interconversion Correlation

State (PG grade)	RAP content (%)	R^2
NH (PG 64 -28)	0	0.7669
	20	0.969
	30	0.3785
	40	0.9838
NY (PG 58 -28)	30	0.9838
	40	0.9654
NY (PG 64 -22)	0	0.8963
	20	0.4517
	30	0.7179
	40	0.8341
VT (PG 52 -34)	0	0.8213
	20	0.7508
	30	0.6929
	40	0.9626
VT (PG 64 -28)	0	0.9327
	20	0.8899
	30	N/A
	40	0.9707

the AASHTO T322-07 (AASHTO 2007) recommendation. A state of plane stress was assumed and the time simulation was set to 3 s. In actual testing conditions, no specimen lasted for more than 2 s. Fig. 4 shows the tensile strain rate profile along the vertical axis of the specimen superimposed over half of the model. The y-axis corresponds to the diameter of the specimen. At the vicinity of the loading strip, one can notice the compressive strains in the horizontal direction.

The average strain rate was found to be 4.45×10^{-4} (ϵ/s); however, for the IDT strength calculations, a constant tensile strain rate of 4.0×10^{-4} (ϵ/s) was used. The value was an average of the tensile strain rates along the specimen's diameter during the test.

Critical Temperature

For the thermal stress restrained specimen test (TSRST) calculations, a fixed rate of cooling, R_T , of 10°C/h was assumed. Considering that the thermal loading starts at time $t = 0$, the rate of thermal strain is given by

$$\frac{d\epsilon_T(t)}{dt} = \alpha R_T \quad (16)$$

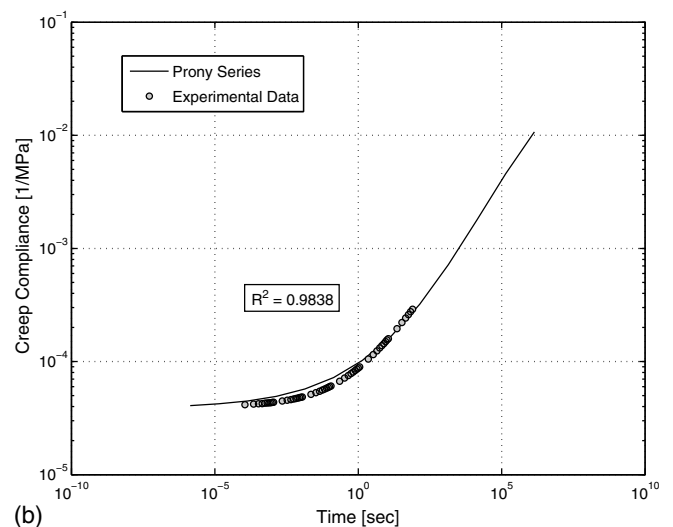
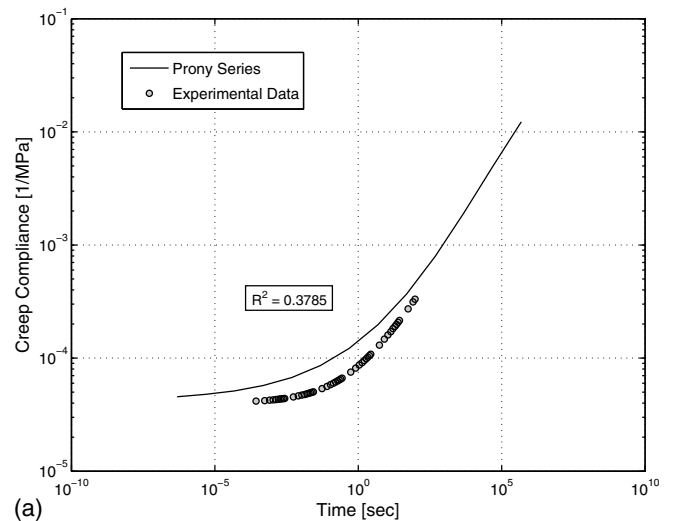


Fig. 5. Comparison between creep compliances: (a) NH PG 64 -28 30 RAP; (b) NY PG 58 -28 30 RAP

The index T in the strain refers to temperature and is used to distinguish it from mechanical strains for the IDT strength analysis.

The analysis of different scenarios was conducted by changing the input variables accordingly. For TSRST stress calculations, the strain rate was obtained from the cooling rate using Eq. (11). The relaxation modulus was shifted to the initial temperature and new Prony coefficients were fit to this curve at that particular temperature. The reduced time was generated based on cooling rates and shift factors. IDT strength values were attained by shifting $E(t)$ to -10°C and applying a load rate of $4.0 \times 10^{-4} (\epsilon/s)$.

The critical cracking temperature could also be established. The calculated IDT strength at -10°C served as the threshold for thermal crack initiation, and the calculated TSRST was used to estimate the stresses in the pavement. The temperature to which the thermal stresses reached the maximum admissible strength is considered to be the critical cracking temperature.

Materials and Methods

The data utilized in this study was generated as part of phase I of the Transportation Pooled Fund TPF - 5 (230) research project, *Evaluation of Plant Produced RAP Mixtures in the Northeast*. This research effort was set forth to examine the effects of different RAP levels on low-temperature and fatigue properties of asphalt mixtures and was conducted on asphalt mixtures designed for service in cold-climate regions. The testing program was carried out at various research centers and involved reclaimed material from three different states. Testing of plant-produced mixtures made it possible to evaluate the impact of higher RAP percentages on material properties and performance with respect to low temperature and fatigue cracking.

Contractors from the states of New Hampshire, New York, and Vermont volunteered to produce mixtures at different RAP contents using six different virgin binders, which totaled 18 distinct mixtures. Mixtures from the state of New York were produced by Callanan Industries in a Cedar Rapids counter flow drum plant. These mixtures were produced at rates of approximately 250 tons per hour [tph] for the 30 and 40% RAP mixtures and 300 tph for the virgin and 20% RAP mixes. Mixtures from the states of New Hampshire and Vermont were produced by Pike Industries in two different facilities. New Hampshire mixtures were produced in a 2008 Gencor Ultra drum plant at a production rate of 400 tph, whereas Vermont mixtures were produced in a 1966 H&B 5-t drop batch plant with mixing times and burner set temperature varying depending on the RAP content. Each facility provided one set of loose mix sampled from the trucks prior to leaving the facility. The loose mixture was stored into 18.9-L (5-gal.) metal buckets for sample fabrication in the lab. Design parameters are shown in Table 1.

The specimens were tested following the experimental plan shown in Table 2. The fatigue tests were executed on an AMPT machine following the protocol proposed by Kim et al. (2009). All the tests were carried out on three replicates of each mix, with the exception of fatigue tests that used only two replicates.

Three expressions used to characterize the temperature dependence of the mixtures were investigated. The polynomial, William-Landel-Ferry (WLF), and exponential models were fit to the dynamic modulus shift factors at a reference temperature of 0°C . The fitted curves were then used to estimate the shift factors at temperatures corresponding to those of the creep compliance test (0, -10 , and -20°C). The predicted values were then compared to actual values and the error between the two calculated. The models

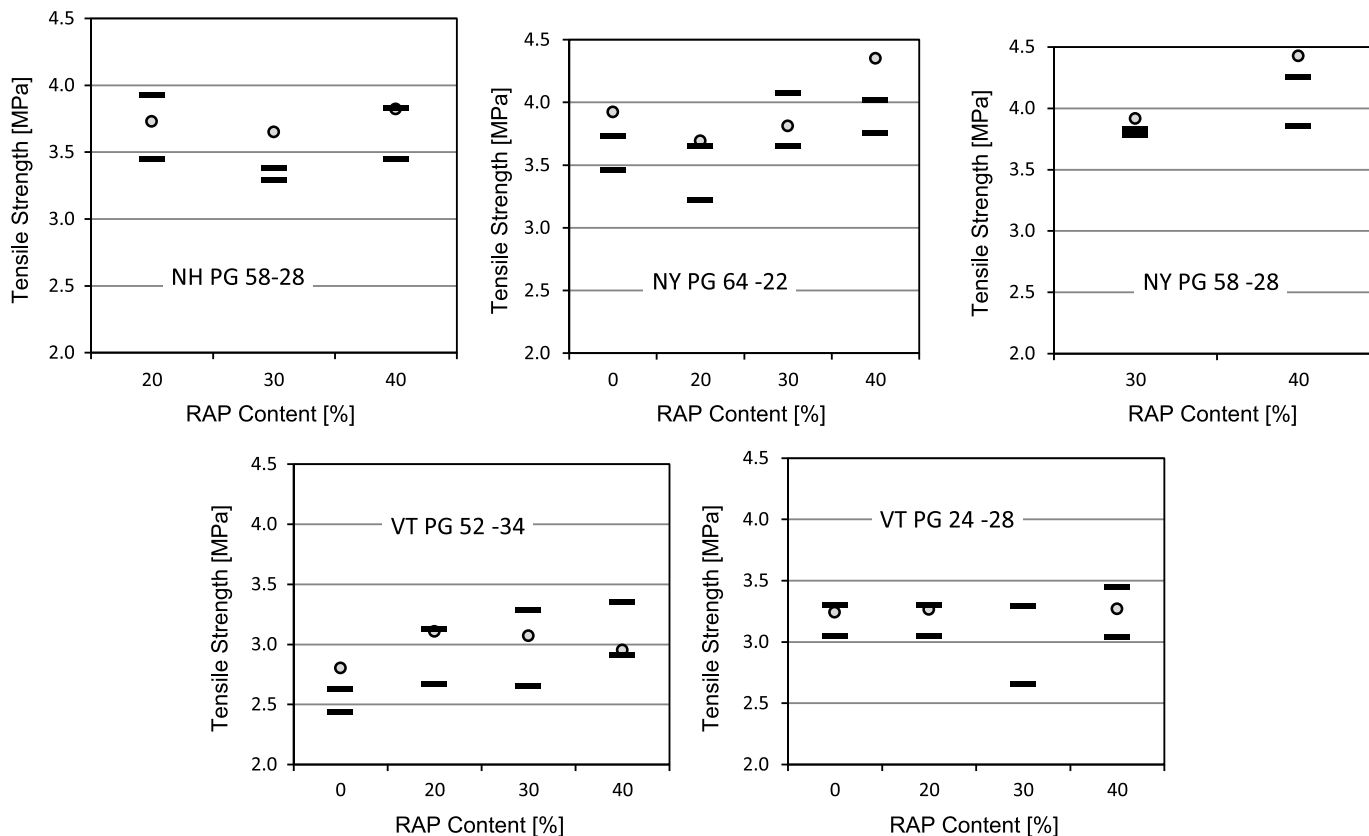
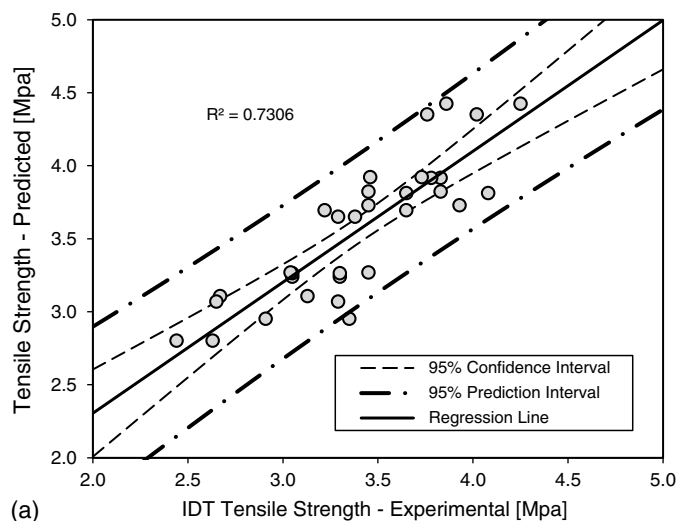
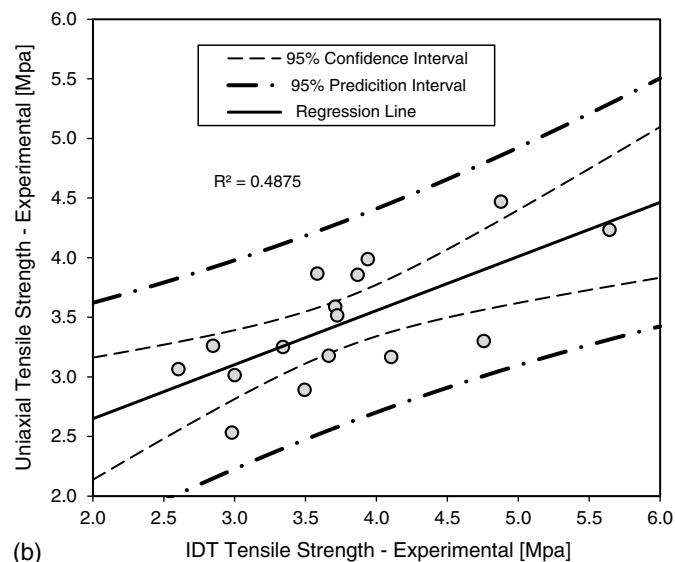


Fig. 6. Predicted tensile strengths versus experimental boundaries



(a) IDT Tensile Strength - Experimental [Mpa]



(b) IDT Tensile Strength - Experimental [Mpa]

Fig. 7. Relationship between IDT and uniaxial strength: (a) experimental versus predicted; (b) experimental versus experimental (data from Christensen and Bonaquist 2004)

used in this work are presented in Table 3, where ΔT is the change in temperature with respect to an arbitrary reference temperature.

Results

Table 4 presents the maximum and minimum errors for the creep compliance shift factors estimation based on dynamic modulus tests. The maximum error usually occurred at -20°C , which may have been caused by changes in the binder microstructure due to the proximity of the glassy state for some mixtures. In overall terms, no significant difference among the three models was found, especially between the polynomial and WLF. In general, the polynomial fit for the shift factor curves of the data set analyzed in this research was found to be the strongest predictor; thus, this model was adopted in this study.

Creep compliance curves interconverted from uniaxial $|E^*|$ mastercurves were calculated and compared against those from IDT creep tests. The correlation between the two data sets was inferred by the coefficient of determination, R^2 , reported in Table 5. Examples of the weakest and strongest correlations are shown in

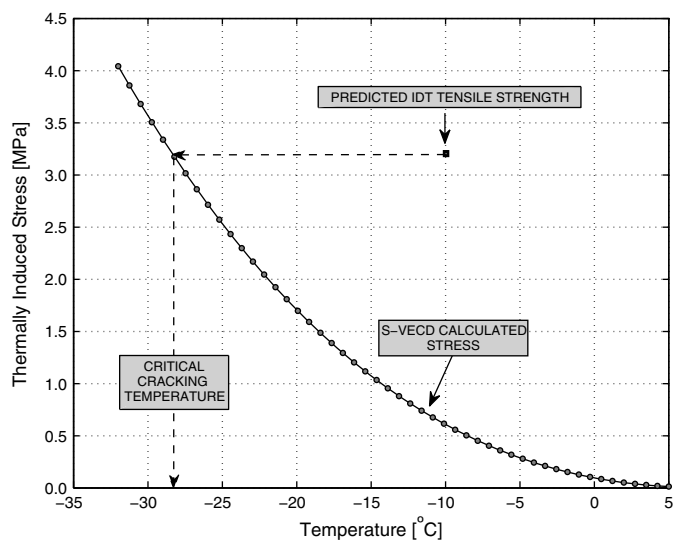


Fig. 8. TSRST thermally induced stress versus IDT strength

Figs. 5(a and b), respectively. A problem in the IDT creep testing of the Vermont PG 64 -28 30 RAP happened during the course of this work. The specimens were damaged due to an operator error; therefore, no data are available for this mix.

The TCMModel calls for two input parameters obtained from the creep compliance curve, namely the initial creep compliance (D_0) and the slope of the linear part of the curve in the log-log scale (m). These two parameters were obtained from the interconverted creep curve and compared to those from the actual creep tests.

The comparisons among the predicted tensile and the experimental IDT strengths are shown in Fig. 6. The dashes are the maximum and minimum values from the three replicates tested. New Hampshire mixtures containing 0% RAP could not be analyzed due a problem in the fatigue characterization of the specimens for that particular mix. In general, the results were satisfactory and within the variability of the test itself.

All the experimental IDT strength results were plotted against the values predicted from the proposed methodology. A linear regression was carried out and the confidence and prediction intervals were estimated for a 95% level. The results are shown in Fig. 7(a), where the solid line represents the best-fit linear curve. Except for one point, all the predicted values fell within the 95% prediction interval. For comparison purposes, the data reported in the NCHRP Project 530 (converted from psi to MPa) is presented in Fig. 7(b).

TSRST was performed according to the AASHTO TP 10-93 (AASHTO 1993) standard, which establishes that the specimen must be cooled down at a rate of 10°C per hour, starting from 5°C until the brittle rupture of the specimen. Fig. 8 illustrates the proposed methodology for critical cracking temperature. It shows the calculated tensile strength threshold and the calculated thermally induced stresses from the TSRST model. The point where the two curves intercept each other was taken as the critical cracking temperature. This criterion will be further validated when the field performance data become available.

Concluding Remarks

The presented method has the virtue of being more amenable to practitioners and time-saving/cost-effective to researchers, therefore adding to the efforts to improve the performance of flexible pavements to thermal cracking. The results showed the applicability

of the proposed methodology to HMA assessment of low-temperature cracking performance. The second-order polynomial yielded the overall best results for shift factor curve fitting as compared to the WLF and exponential models.

A strong correlation was observed between the IDT strength calculated using the VECD model and the measured values. No constraints regarding the use of the proposed methodology was found when RAP mixes were analyzed. The interconversion from dynamic modulus to creep compliance using the results from an AMPT device helps to decrease the time and effort consumed in the characterization of HMA mixtures at low temperature.

This work is believed to be a pioneer in the use of an advanced constitutive modeling to assess the low-temperature cracking performance of high RAP mixtures. It also contributes to a better understanding of the impacts of adding reclaimed material to virgin mixtures. Moreover, this study provides an important tool to help the design of new pavements as well as the distress prediction and rehabilitation planning of the existing highway infrastructure of cold-climate regions.

References

- AASHTO. (1993). "Standard test method for thermal stress restrained specimen tensile strength." *TP10-93*, Washington, DC.
- AASHTO. (2007). "Standard method of test for determining the creep compliance and strength of hot-mix asphalt (HMA) using the indirect tensile test device." *T322-07*, Washington, DC.
- AASHTO. (2012). "Standard method of test for determining the dynamic modulus and flow number for hot mix asphalt (HMA) using the asphalt mixture performance tester (AMPT)." *TP79-12*, Washington, DC.
- ABAQUS version 6.11 [Computer software]. RI, Dassault Systems.
- Bonaquist, R. F., Christensen, D. W., and Stump, W. (2003). "Simple performance tester for Superpave mix design: First-article development and evaluation." *NCHRP Rep. 513*, Washington, DC.
- Chehab, G. R., and Kim, R. Y. (2005). "Viscoelastoplastic continuum damage model application to thermal cracking of asphalt concrete." *J. Mater. Civ. Eng.*, 10.1061/(ASCE)0899-1561(2005)17:4(384), 384–392.
- Christensen, D. W., and Bonaquist, R. F. (2004). "Evaluation of indirect tensile test (IDT) procedures for low-temperature performance of hot mix asphalt." *NCHRP Rep. 530*, National Cooperative Highway Research Program, Washington, DC.
- Christensen, R. M. (1982). *Theory of viscoelasticity*, 2nd Ed., Academic Press, New York.
- Cost, T. L., and Becker, E. B. (1970). "A multidata method of approximate Laplace transform inversion." *Int. J. Numer. Method. Eng.*, 2(2), 207–219.
- Daniel, J. S. (2001). "Development of a simplified fatigue test and analysis procedure using a viscoelastic continuum damage model and its application to WesTrack mixtures." North Carolina State Univ., Raleigh, NC.
- Haas, R., Meyer, F., Assaf, G., and Lee, H. (1987). "A comprehensive study of cold climate airport pavement cracking." *J. Assoc. Asphalt Paving Technol.*, 56, 198–245.
- Hiltunen, D. R., and Roque, R. (1994). "A mechanics-based prediction model for thermal cracking of asphaltic concrete pavements." *J. Assoc. Asphalt Paving Technol.*, 63, 81–108.
- Jones, G. M., Darter, M. I., and Littlefield, G. (1968). "Thermal expansion-contraction of asphaltic concrete." *J. Assoc. Asphalt Paving Technol.*, 37, 56–97.
- Kim, H., Wagoner, M. P., and Buttlar, W. G. (2008). "Simulation of fracture behavior in asphalt concrete using a heterogeneous cohesive zone discrete element model." *J. Mater. Civ. Eng.*, 10.1061/(ASCE)0899-1561(2008)20:8(552), 552–563.
- Kim, R. Y., Guddati, M. N., Underwood, S. B., Yun, T. Y., Subramanian, V., and Savadatti, S. (2009). "Development of a multiaxial viscoelastoplastic continuum damage model for asphalt mixtures." *FHWA-HRT-08-073*, FHWA, Georgetown Pike, VA.
- Kreyszig, E. (2011). *Advanced engineering mathematics*, 10th Ed., Wiley, New York.
- Mun, S. (2006). "Numerical computation of convolution integral for the linear viscoelasticity of asphalt concrete." *KSCCE J. Civ. Eng.*, 10(3), 195–200.
- Paris, P. C., Gomez, M. P., and Anderson, W. E. (1961). "A rational analytic theory of fatigue." *Trend Eng.*, 13, 9–14.
- Park, S. W., Kim, R. Y., and Schapery, R. A. (1996). "A viscoelastic continuum damage model and its application to uniaxial behavior of asphalt concrete." *Mech. Mater.*, 24(4), 241–255.
- Park, S. W., and Schapery, R. A. (1997). "A viscoelastic constitutive model for particulate composites with growing damage." *Int. J. Solid. Struct.*, 34(8), 931–947.
- Park, S. W., and Schapery, R. A. (1999). "Methods of interconversion between linear viscoelastic material functions. Part I—A numerical method based on Prony series." *Int. J. Solid. Struct.*, 36(11), 1653–1675.
- Schapery, R. A. (1975). "A theory of crack initiation and growth in viscoelastic media. I. Theoretical development." *Int. J. Fract.*, 11(1), 141–159.
- Taylor, R. L., Pister, K. S., and Goudreau, G. L. (1970). "Thermomechanical analysis of viscoelastic solids." *Int. J. Numer. Method. Eng.*, 2(1), 45–59.
- Underwood, S. B., Hou, E. T., and Kim, R. Y. (2009). "Advanced testing and characterization of bituminous materials." Chapter 82, *Application of simplified VECD modeling to the fatigue life prediction of asphalt concrete mixtures*, L. Andreas, M. Partl, T. Scarpas, and I Al-Qadi, eds., CRC Press.
- Underwood, S. B., and Kim, R. Y. (2011). "Viscoelastoplastic continuum damage model for asphalt concrete in tension." *J. Eng. Mech.*, 10.1061/(ASCE)EM.1943-7889.0000277, 732–739.
- Wagoner, M. P., Buttlar, W. G., and Paulino, G. H. (2005). "Development of a single-edge notched beam test for asphalt concrete mixtures." *J. Test. Eval.*, 33(6), 452–460.
- Zocher, M. A., Groves, S. E., and Allen, D. H. (1997). "A three-dimensional finite element formulation for thermoviscoelastic orthotropic media." *Int. J. Numer. Method. Eng.*, 40(12), 2267–2288.